WASHINGTON UNIVERSITY

Department of Physics

St. Louis 5, Missouri

TECHNICAL REPORT No. [illegible]

114. THE TRANSMISSION OF ELECTRONS THROUGH THIN METALLIC FOILS - C. N. Chang, C. S. Cook, H. Primakoff

115. PSEUDOSCALAR INTERACTION IN THE THEORY OF BETA-DECAY - H. [illegible]

116. ANGULAR CORRELATION BETWEEN THE FIRST AND THIRD GAMMA RAYS IN Ti[illegible] - C. E. Whittle, P. [illegible]

117. PROTON-DEUTERON SCATTERING AT [illegible] MEV AND DEUTERON-PROTON SCATTERING AT 10.2 MEV. - K. B. [illegible]

DECEMBER 16, 195[illegible]

CONTRACT N6 ORI-117, TASK ORDER I
(Nuclear Physics)

with

OFFICE OF NAVAL RESEARCH

U. S. NAVY DEPARTMENT

RDB No. NR 024-018

Technical Report No. 114

December 16, 1953

THE TRANSMISSION OF ELECTRONS THROUGH THIN METALLIC FOILS

By

C. H. Chang, C. S. Cook

and H. Primakoff

Reprinted from THE PHYSICAL REVIEW, Vol. 90, No. 4, 544–547, May 15, 1953
Printed in U. S. A.

The Transmission of Electrons through Thin Metallic Foils*

C. H. CHANG, C. S. COOK, AND H. PRIMAKOFF
Physics Department, Washington University, St. Louis, Missouri

(Received December 12, 1952)

Experimental studies have been made on the relative transmission of positrons and negatrons in the energy range 50-750 kev through aluminum and platinum windows of an end-window-type G-M counter. In qualitative agreement with the theoretical predictions that more scattering takes place in material having higher atomic number, a platinum foil having the same surface density as a corresponding aluminum foil shows lower relative transmission at any given energy even though the low energy cutoffs of the two windows are just about the same. Also in qualitative agreement with theory, a larger percentage of positrons than negatrons are transmitted at any given energy for the same platinum foil. Theoretical transmission curves, with an empirically determined constant, have been developed. These curves are in relatively good agreement with the experimental curves.

I. INTRODUCTION

FROM the point of view of the beta-ray spectroscopist studying nuclear beta- and gamma-ray spectra, a Geiger-Müller counter window introduces experimental distortions in the magnitudes and shapes of low energy spectra. In practice, methods have been devised either for the measurement of the transmission coefficient of the counter window[1–3] in order to correct for this effect, or, attempts have been made to eliminate the counter window entirely.[4] From a more fundamental aspect, however, the problem is actually a form of the general problem of the passage of electrons through matter which has been a subject of much study since the first discovery of cathode rays and which has recently been investigated intensively[5–10] in the range of energies considered in this paper. If attacked from this point of view, the transmission coefficient η of a G-M counter window foil may be considered as consisting of two parts which we shall call η_E and η_I. The quantity η_E is a measure of the amount of elastic scattering of the electrons within the foil. The elastic scattering is important, since some of the electrons do not pass completely through the foil and get into the sensitive region of the G-M counter because they are scattered through too large an angle to enter this region. The second quantity η_I is a measure of the inelastic scattering between the passing electron and the atoms of the foil; such inelastic scattering may lead to the actual stopping of the electron within the foil. The total coefficient is the product of these two parts ($\eta=\eta_E\eta_I$). Actually, of course, these two quantities are not entirely statistically independent one from the other, but handling them as separate entities appears valid in first approximation and leads to reasonably good results.

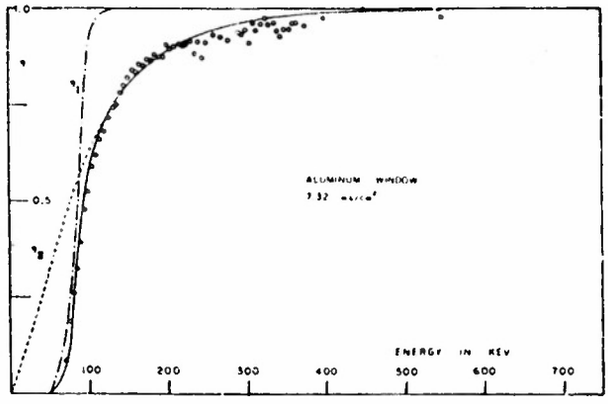

FIG. 1. Relative electron transmission η through a 7.32 mg/cm² aluminum G-M counter window as a function of the electron's incident kinetic energy. In this and subsequent figures the circles represent experimentally determined negatron transmissions, and the plus signs experimentally determined positron transmissions. The continuous line is the theoretical transmission coefficient, $\eta=\eta_E\eta_I$, as determined by the method discussed in the text. To show the relative importance of η_E and η_I at various energies the theoretically determined curves for these two quantities are also shown in this diagram.

II. EXPERIMENTAL RESULTS

The measurements made in the current experiments on the relative transmission of negatrons and positrons through various aluminum and platinum G-M counter windows are indicated in Figs. 1 through 5. These represent seven sets of data, since two of the figures give results for both positrons and negatrons for the same window. The solid lines represent a type of theoretical curve which will be discussed in the next section.

The experimental measurements were performed on the lens spectrometer previously used[3] for this purpose. However, the experimental data presented here were not obtained by means of the acceleration technique[3] but were obtained through a comparison method. Since all aluminum and platinum windows used for the cur-

* Assisted by the joint program of the U. S. Office of Naval Research and the U. S. Atomic Energy Commission.

[1] D. Saxon, Phys. Rev. **81**, 639 (1951).
[2] Heller, Sturcken, and Weber, Rev. Sci. Instr. **21**, 898 (1950).
[3] C. H. Chang and C. S. Cook, Nucleonics **10**, No. 4, 24 (1952).
[4] Langer, Motz, and Price, Phys. Rev. **77**, 798 (1950).
[5] Groetzinger, Humphrey, and Ribe, Phys. Rev. **85**, 78 (1952).
[6] H. J. Lipkin, Phys. Rev. **85**, 517 (1952).
[7] H. H. Seliger, Phys. Rev. **88**, 408 (1952).
[8] Christian, Dunning, and Martin, Nucleonics **10**, No. 5, 41 (1952).
[9] W. Paul and H. Reich, Z. Physik **131**, 326 (1952).
[10] E. Hisdal, Phil. Mag. **43**, 790 (1952).

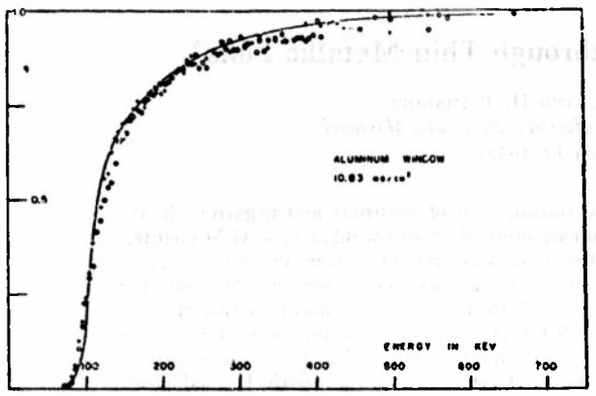

FIG. 2. Relative electron transmission η through a 10.83-mg/cm² aluminum window. See caption for Fig. 1 for explanation.

rent experiment are relatively thick, as G-M counter windows go, a thin Zapon window will transmit, within experimental error, 100 percent of the beta-particles at the energies under consideration. For this reason one can obtain spectra for the negatrons (Ag^{110}) and for the positrons (Cu^{61}) using a thin Zapon window and, by comparison with the spectra obtained using the thicker metallic windows, calculate a relative transmission curve for these thicker windows. This method could be applied quite simply to the Ag^{110} negatron source since its long half-life allowed the same source to be used for all measurements (with appropriate decay corrections). However, the short half-life of the Cu^{61} positron source forced the preparation of a new source for each set of data. The preparation of a Cu^{61} source has been, however, so standardized that it was possible to prepare two or more such sources almost identical one with the other. Corrections were made for small variations in the intensity of the different sources through comparison of the sources with a standard long-lived source under conditions of a standardized geometry.

When it can be applied and when measurements must be made on a number of different sources, the comparison method requires less expenditure of time than does the acceleration technique. However, slight discrepancies between the two techniques still appear in the energy region just above the window cutoff.

III. THE ELASTIC TRANSMISSION COEFFICIENT η_E

Monoenergetic electrons entering a foil may be elastically scattered through any (total) angle, depending upon the number of individual collisions between them and the atoms of foil and upon the angles of scattering in these collisions. The distribution of the electrons upon leaving the foil will be some function $P(\theta)$ of the (total) spatial angle of multiple scattering θ. The form of this function will depend upon the geometrical thickness L_0, the number density of the atoms in the foil N/V, the type of foil material (atomic number Z), the kinetic energy of the incident electrons E, and the polarity of the electron charge (negatrons, $Z'e=-e$, or positrons $Z'e=+e$). The elastic transmission coefficient η_E can then be expressed as

$$\eta_E=\int_0^{\theta_{max}} P(\theta)d\theta, \tag{1}$$

where θ_{max} is the maximum (total) angle through which an electron may be scattered by the G-M counter window foil and still enter the sensitive region of the G-M counter. For ease in calculation we shall normalize $P(\theta)$ in the interval $0\leq\theta<\infty$, even though physically $0\leq\theta<\pi$, since the form of $P(\theta)$ which we shall use is small for $\pi\leq\theta<\infty$.

In the present paper we will not attempt to derive the actual form of $P(\theta)$ from basic theoretical considerations. However, we will show that the crude assumption of a decreasing exponential function of θ for the scattering probability per unit solid angle will lead to results for η_E which can be brought into approximate agreement with the experimental observations. Such a normalized function is

$$P(\theta)d\theta=\alpha^2\exp(-\alpha\theta)\sin\theta d\theta\approx\alpha^2\exp(-\alpha\theta)\theta d\theta, \tag{2}$$

the choice of this function being initially justified on the basis that it is a simple function which at least roughly resembles the spatial distribution associated with the projected "Gaussian" plus "tail" distribution which has been used in most "small angle" multiple scattering theories. From Eqs. (1) and (2) one then obtains

$$\eta_E=1-\{\exp(-\alpha\theta_{max})\}\{1+\alpha\theta_{max}\},$$

with α determined via the mean square angle of multiple scattering by

$$\langle\theta^2\rangle=\int_0^{\pi}\theta^2P(\theta)d\theta=6/\alpha^2,$$

$$\alpha=2.45/\langle\theta^2\rangle^{\frac{1}{2}}. \tag{3}$$

There then remains only one arbitrary constant within the equation for η_E, namely, θ_{max}; for our counter ge-

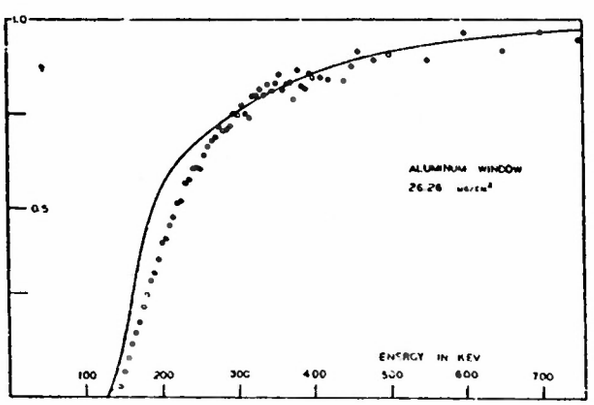

FIG. 3. Relative electron transmission η through a 26.26-mg/cm² aluminum window. See caption for Fig. 1 for explanation.

ometry, the assumption of $\theta_{max}=1$ radian appears reasonable. Thus, the equation from which η_E has to be determined for each window becomes

$$\eta_E=1-\{\exp[-2.45/\langle\theta^2\rangle^{\frac{1}{2}}]\}\{1+2.45/\langle\theta^2\rangle^{\frac{1}{2}}\}. \quad (4)$$

The mean square angle of multiple scattering can now be found (in the "small angle" approximation) from an expression involving the single scattering probability distribution through an angle ϕ.[11] Using, in addition, in this expression a "spin orbit correction" factor $\gamma(\phi)$,[12] we obtain a formula for the mean square angle of multiple scattering,

$$\langle\theta^2\rangle=\frac{8\pi NL_0}{V}\left(\frac{ZZ'e^2}{pv}\right)^2\int_0^{\pi/2}\frac{\phi^2\gamma(\phi)d\phi}{\{\phi^2+\phi_{min}^2\}^{\frac{1}{2}}}. \quad (5)$$

Here the foil contains NL_0/V atoms per unit area; p and $v=\beta c$ are, respectively, the momentum and velocity of the incident electron;

$$\phi_{min}=\{1.14mcZ^{\frac{1}{3}}/137p\}\{1.13+3.76(ZZ'/137\beta)^2\}^{\frac{1}{2}},$$

and for small angles,

$$\gamma(\phi)=1-\beta^2\left(\frac{\phi}{2}\right)^2-[\pi ZZ'\beta/137](\phi/2)[1-\phi/2].$$

Actually, for large Z, higher powers of $ZZ'/137$ than the first contribute to $\gamma(\phi)$, but these contributions are relatively unimportant at the rather small ϕ which make the major contribution[13] to $\langle\theta^2\rangle$.

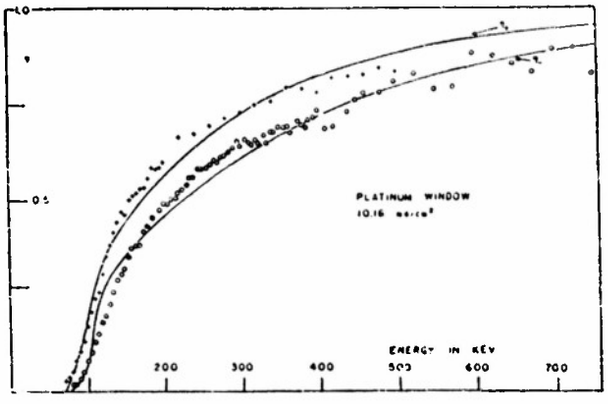

FIG. 4. Relative electron transmission η through a 10.16-mg/cm² platinum window. See caption to Fig. 1 for explanation. The theoretical transmission coefficient designated by the symbol η_+ is the one determined for positrons and that designated by the symbol η_- is the one determined for negatrons.

[11] G. Molière, Z. Naturforsch. **2a**, 133 (1947); **3a**, 78 (1948); S. Olbert, Phys. Rev. **87**, 319 (1952).

[12] W. A. McKinley and H. Feshbach, Phys. Rev. **74**, 1759 (1948); H. Feshbach, Phys. Rev. **88**, 295 (1952).

[13] We neglect the contribution to $\langle\theta^2\rangle$ for values of ϕ between $\pi/2$ and π. In this region both the Rutherford factor in Eq. (5) and the spin orbit correction factor are not accurately given by our very approximate expressions, but we may nevertheless estimate that the net contribution from this region in the integration over the correct single scattering distribution is small compared to the net contribution of the region between $\theta=0$ and $\theta=\pi/2$.

IV. THE INELASTIC TRANSMISSION COEFFICIENT η_I

The inelastic transmission coefficient is determined by the number of electrons which are stopped in the foil. Physically known quantities make it easier to calculate the number of electrons which are stopped rather than the number which penetrate the foil. Therefore it seems appropriate to define a quantity $\eta_S=1-\eta_I$ which represents the probability that an electron is stopped in the foil.

If an electron possessing a fairly high kinetic energy enters a piece of material having semi-infinite extent, it will continue to move until it has been robbed of essentially all its kinetic energy as a consequence of inelastic collisions involving the ionization and excitation of the atoms of the material. The total distance X (effective path length) which the electron travels before stopping will not be the same in all individual cases but will instead be distributed according to a probability function $P_S(X)$ which is in first approximation Gaussian:

$$P_S(X)dX=\exp(-y^2/2\langle y^2\rangle)dy/(2\pi\langle y^2\rangle)^{\frac{1}{2}}.$$

Here $y=X-R$, $\langle X\rangle=R$ is the range of the electron within the material, and $\langle y^2\rangle$, the mean square range straggling, is in first approximation,[14]

$$\langle y^2\rangle=(\langle X-R)^2\rangle=R^2/2\ln(E/I)$$
$$=E^4/32\pi^2(N/V)^2Z^2e^8[\ln(E/I)]^2,$$

where E is the kinetic energy of the incident electron and I is the average ionization energy (we use $13.6Z$ ev for this energy). The actual small difference between the R and the $\langle y^2\rangle$ values for (nonrelativistic) negatrons and for (nonrelativistic) positrons of a given energy is neglected. We then have

$$\eta_I=1-\eta_S=1-\int_0^L P_S(X)dX$$
$$=1-\{1/(2\pi\langle y^2\rangle)^{\frac{1}{2}}\}\int_{-R}^{L-R}\exp(-y^2/2\langle y^2\rangle)dy$$
$$=\tfrac{1}{2}-\{1/(2\pi\langle y^2\rangle)^{\frac{1}{2}}\}\left\{\int_0^{L-R}\exp(-y^2/2\langle y^2\rangle)dy\right.$$
$$\left.-\int_R^{\infty}\exp(-y^2/2\langle y^2\rangle)dy\right\}, \quad (7)$$

where L is the effective path length of an electron

[14] See, for example, H. W. Lewis, Phys. Rev. **85**, 20 (1952). Justification for the use of Lewis' theory of range and of range straggling for a *nonrelativistic* charged particle (negatron or positron) is based upon the fact that η_I affects only the lower energy portion of the transmission curve (see Fig. 1). For higher relativistic electron energies η_I is approximately unity and the transmission curve is determined solely from η_E.

traversing the foil. Using the results of Yang,[15] one has roughly, $L=(1+\langle\theta^2\rangle/4)L_0$; also, the second integral [in the last form of Eq. (7)] can be dropped since $R/(2\langle y^2\rangle)^{\frac{1}{2}}=[\ln(E/I)]^{\frac{1}{2}}\gg 1$, while the first integral can be found from available tables[16] and graphs.[17]

The results of these calculations for η_I, as well as those for η_E and the combined result $\eta=\eta_E\eta_I$, are shown for the 7.32-mg/cm² aluminum window in Fig. 1. Other graphs for the remaining windows show only the final theoretical result $\eta=\eta_E\eta_I$.

V. DISCUSSION

It will be noted that $\langle\theta^2\rangle$ plays a very important role in the present work, since it is instrumental in the determination of both η_E and η_I. Because of this use of the "scattering" approach to the problem of window transmission, it is valid to compare our results with those made through the study of the scattering by various materials of electrons in the energy range considered here (from about 30 kev to a few Mev). Qualitatively the results agree.

Our results show that, in a high Z material—platinum, at a given energy, the transmission coefficient for positrons is greater than for negatrons; in agreement with the observations[5–7] that there is a greater single scattering of negatrons than positrons at high Z. In addition, for a given foil surface density, the transmission coefficient for aluminum is greater than for platinum, in agreement with the observations[7,8] that the amount of single scattering increases with larger atomic number of the scattering material.

For comparison of our distribution function [Eq. (2)] with the measurements of Hisdal[10] on the scattering of 0.5-Mev electrons in an Ilford G5 emulsion, we must transform our distribution for spatial angles into an equivalent form for projected angles. Such a transformation shows that the projected distribution is approximately proportional to $\exp(-\alpha|\Theta|)[|\Theta|+1/\alpha]$ where Θ is the projected scattering angle. Using the data for Ilford G5 emulsions, as given by Voyvodic and Pickup,[18] and the cell length given by Hisdal, to determine α, our distribution is in rough agreement with Hisdal's experimental results.

[15] C. N. Yang, Phys. Rev. 84, 599 (1951). This formula is, however, applicable only to small angles.

[16] *Table of Probability Functions*, prepared by Federal Works Agency, Works Project Administration, sponsored by National Bureau of Standards, 1941.

[17] E. Jahnke and F. Emde, *Tables of Functions* (Dover Publications, New York, 1945), fourth edition, pp. 23–25.

[18] L. Voyvodic and E. Pickup, Phys. Rev. 85, 91 (1952).

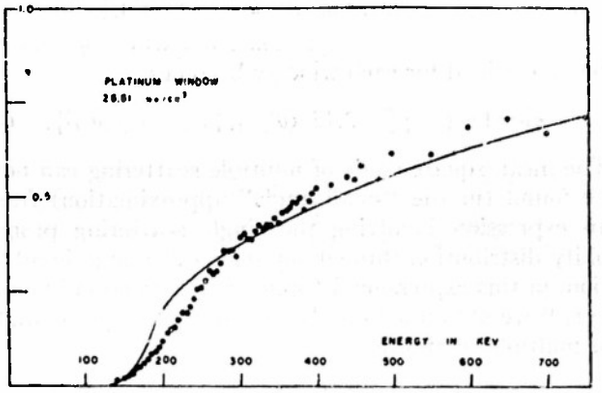

FIG. 5. Relative electron transmission η through a 25.51-mg/cm² platinum window. See caption to Fig. 1 for explanation.

As has already been mentioned, the distribution function for multiple elastic scattering used in the present calculations is of the same general shape in its "small angle" plane projected form as the more commonly used sum of a "Gaussian" plus "tail." Apart from this, possibly the only virtue of our distribution is its simplicity for numerical calculations. Considering this and the number of additional approximations which have been made in the determination of η_E and η_I, the theoretically determined curves for η are in not unsatisfactory agreement with the experimental observations.

These approximations, it will be recalled, are as follows: (a) the omission of any systematic treatment of the inelastic collision energy losses in the treatment of the multiple elastic scattering and the parallel omission of the effect of multiple elastic scattering in the treatment of the stopping probability due to inelastic collision;[19] (b) the use of a crude "small angle" exponential approximation to the "Gaussian" plus "tail" "small angle" multiple scattering distribution in a physical situation where some of the angles of multiple scattering become quite appreciable; and (c) the use of very approximate expressions for the electron range and range straggling. In spite of these perhaps mutually compensating approximations, the agreement between theory and experiment seems to indicate that a future rigorous calculation of the transmission coefficient η should yield results not too different from those developed here.

[19] Except in so far as our use of the approximate relation between I and I_0.

Technical Report No. 115

December 16, 1953

PSEUDOSCALAR INTERACTION IN THE THEORY OF BETA-DECAY. II

By

Tino Ahrens

Reprinted from THE PHYSICAL REVIEW, Vol. 90, No. 5, 974-977, June 1, 1953
Printed in U. S. A.

Pseudoscalar Interaction in the Theory of Beta-Decay. II*

TINO AHRENS†
Washington University, St. Louis, Missouri
(Received February 24, 1953)

It is shown that analysis of the pseudoscalar interaction in beta-decay theory results in the appearance of the two sets of nuclear matrix elements,

$$\int \theta_p \beta\gamma_5 \quad \text{and} \quad \frac{i}{2M}\int \theta_p \boldsymbol{\sigma}\cdot\{\nabla\},$$

θ_p denoting the angular part of the pseudoscalar lepton covariant and $\{\nabla\}$ the gradient operation on the radial part of this covariant, instead of the single matrix element,

$$\int \theta_p \gamma_5.$$

As a consequence pseudoscalar interaction correction factors containing derivatives of the lepton wave functions are deduced.

1. INTRODUCTION

IN the theory of beta-decay, the transition probability is

$$P(W)dW=(1/2\pi^3)FCW(W_0-W)^2(W^2-1)^{\frac{1}{2}}dW, \quad (1)$$

with the Fermi function

$$F=4(2p\rho)^{2(s-1)}e^{\pi\delta}|\Gamma(s+i\delta)|^2/\Gamma^2(2s+1), \quad (2)$$
$$\delta=ZW/137p, \quad s^2=1-(Z/137)^2,$$

and the correction factor

$$C=2\pi|ME|^2/F(W^2-1), \quad (3)$$

where

$$ME=\sum_N(f|H_{\text{int}N}|i)\equiv(f|H_{\text{int}}|i) \quad (4)$$

denotes the transition matrix element,

$$H_{\text{int}N}=\{G_s\beta_N\psi^\dagger\beta\varphi+G_v[1_N\psi^\dagger 1\varphi-\boldsymbol{\alpha}_N\cdot\psi^\dagger\boldsymbol{\alpha}\varphi]$$
$$+G_t[(\beta\boldsymbol{\sigma})_N\cdot\psi^\dagger\beta\boldsymbol{\sigma}\varphi+(\beta\boldsymbol{\alpha})_N\cdot\psi^\dagger\boldsymbol{\alpha}\varphi]$$
$$+G_a[\boldsymbol{\sigma}_N\cdot\psi^\dagger\boldsymbol{\sigma}\varphi-\gamma_{5N}\psi^\dagger\gamma_5\varphi]$$
$$+G_p(\beta\gamma_5)_N\psi^\dagger\beta\gamma_5\varphi\}Q_N \quad (5)$$

the interaction Hamiltonian for the Nth nucleon, Q_N the charge coordinate transformation operator for the Nth nucleon, and ψ and φ, respectively, the electron and neutrino wavefunctions evaluated at the position of the Nth nucleon; the sum $\sum_N$ is to be extended over all nucleons; $G_{s,v,t,a,p}$ are the scalar, vector, tensor, axial vector, and pseudoscalar coupling constants.

2. THEORY

The following procedure is adopted for the evaluation of the pseudoscalar transition matrix element,

$$ME_p=(f|\beta\gamma_5 L_p|i),$$

($\beta\gamma_5$ is here the abbreviation for $G_p\sum_N(Q\beta\gamma_5)_N$, and L_p for $\psi^\dagger\beta\gamma_5\varphi$): Subtract an initial state many-nucleon Dirac equation from a Hermitian conjugate final state many-nucleon Dirac equation after the first has been multiplied from the left by $\psi_f^\dagger\sum_N(Q\gamma_5)_N L_p$ and the second from the right by $\sum_N(Q\gamma_5)_N L_p\psi_i$. Integration and rearrangement then yields

$$2M(f|\beta\gamma_5 L_p|i)=(W_i-W_f)(f|\gamma_5 L_p|i)$$
$$+i(f|\boldsymbol{\sigma}\cdot\{\nabla L_p\}|i)+(f|[V,\gamma_5 L_p]|i), \quad (6)$$

where V is a perfectly general internucleon potential energy operator and W_i, W_f are initial and final state energy eigenvalues. Evaluating the radial part R_p of the lepton covariant L_p at the nuclear boundary ρ wherever possible, transforms Eq. (6) into

$$2M(f|\beta\gamma_5 L_p|i)\cong(W_i-W_f)(f|\gamma_5\theta_p|i)R_p]_\rho$$
$$+i(f|\boldsymbol{\sigma}\cdot\{\nabla\theta_p\}|i)R_p]_\rho+i(f|\theta_p\boldsymbol{\sigma}\cdot\{\nabla|i)R_p\}_\rho$$
$$+(f|[V,\gamma_5\theta_p]|i)R_p]_\rho+(f|\gamma_5\theta_p[V,R_p]|i). \quad (7)$$

But in a similar way,

$$2M(f|\beta\gamma_5\theta_p|i)\cong(W_i-W_f)(f|\gamma_5\theta_p|i)$$
$$+i(f|\boldsymbol{\sigma}\cdot\{\nabla\theta_p\}|i)+(f|[V,\gamma_5\theta_p]|i), \quad (8)$$

whence, multiplying (8) by $R_p]_\rho$ and subtracting the result from (7),

$$ME_p=(f|\beta\gamma_5 L_p|i)\cong(f|\beta\gamma_5\theta_p|i)R_p]_\rho$$
$$+(i/2M)(f|\theta_p\boldsymbol{\sigma}\cdot\{\nabla|i)R_p\}_\rho$$
$$+(1/2M)(f|\gamma_5\theta_p[V,R_p]|i). \quad (9)$$

The analysis thus leads, assuming sufficiently small velocity dependence in V, to the two sets of nuclear matrix elements in the expression for ME_p

$$\int\theta_p\beta\gamma_5 \quad \text{and} \quad \frac{i}{2M}\int\theta_p\boldsymbol{\sigma}\cdot\{\nabla\}, \quad (10)$$

* Assisted by the joint program of the U. S. Office of Naval Research and the U. S. Atomic Energy Commission. The article contains part of a thesis submitted in partial fulfilment of the requirements for the Ph.D. degree, obtained under a U. S. Atomic Energy Commission predoctoral fellowship.
† Now at Convair, Fort Worth, Texas.

TABLE I. Correction factors for parity change transitions: $\Delta I=0$ (yes).

$$G_v'\left\{\left|\int \boldsymbol{\sigma}\cdot\mathbf{r}\right|^2\left\{\frac{g_0'^2+f_{-2}'^2}{\rho^2}-\frac{2K}{3}\left[\frac{(f_0+f_0'\rho)g_0'-(g_{-2}+g_{-2}'\rho)f_{-2}'}{\rho^2}\right]+\frac{K^2}{9}\left[\frac{(f_0+f_0'\rho)^2+(g_{-2}+g_{-2}'\rho)^2}{\rho^2}-\frac{6(g_0g_0'+f_{-2}f_{-2}')}{\rho}-3(g_0'^2+f_{-2}'^2)\right]\right\}\right.$$
$$+2i\int\boldsymbol{\sigma}\cdot\mathbf{r}\left(\int\beta\gamma_5\right)^*\left\{\frac{g_0g_0'+f_{-2}f_{-2}'}{\rho}-\frac{K}{3}\left[\frac{(f_0+f_0'\rho)g_0-(g_{-2}+g_{-2}'\rho)f_{-2}}{\rho}+(f_0g_0'-f_{-2}'g_{-2})\right]\right.$$
$$\left.\left.+\frac{K^2}{}[(f_0+f_0'\rho)f_0+(g_{-2}+g_{-2}'\rho)g_{-2}-3(g_0^2+f_{-2}^2)-3(g_0g_0'+f_{-2}f_{-2}')\rho]\right\}2M\right.$$
$$\left.+\left|\int\beta\gamma_5\right|^2\left\{(g_0^2+f_{-2}^2)-\frac{2K}{3}(f_0g_0-f_{-2}g_{-2})\rho+\frac{K^2}{9}[(f_0^2+g_{-2}^2)\rho^2-3(g_0^2+f_{-2}^2)\rho^2]\right\}4M^2\right\}=C_{pp}{}^{10}\cdot 2p^2F.$$

$$2G_aG_p'\left\{\left|\int\boldsymbol{\sigma}\cdot\mathbf{r}\right|^2\left\{\frac{f_0g_0'+f_{-2}'g_{-2}}{\rho^2}-\frac{K}{3}\left[\frac{g_0g_0'-f_{-2}f_{-2}'}{\rho}-+\frac{(f_0+f_0'\rho)f_0-(g_{-2}+g_{-2}\rho)g_{-2}}{3\rho^2}\right]\right\}+i\int\boldsymbol{\sigma}\cdot\mathbf{r}\left(\int\beta\gamma_5\right)^*\left\{\frac{f_0g_0+f_{-2}g_{-2}}{\rho}\right.\right.$$
$$\left.-\frac{K}{3}[(g_0^2-f_{-2}^2)+\tfrac{1}{3}(f_0^2-g_{-2}^2)]\right\}2M+i\int\gamma_5\left(\int\boldsymbol{\sigma}\cdot\mathbf{r}\right)^*\left\{-\frac{g_0g_0'-f_{-2}f_{-2}'}{\rho}+\frac{K}{3}\left[\frac{(f_0+f_0'\rho)g_0+(g_{-2}+g_{-2}'\rho)f_{-2}}{\rho}-(f_0g_0'+f_{-2}'g_{-2})\right]\right\}$$
$$\left.+\int\gamma_5\left(\int\beta\gamma_5\right)^*(g_0^2-f_{-2}^2)2M\right\}=C_{ap}{}^{10}\cdot 2p^2F.$$

$$2G_tG_p'\left\{\left|\int\boldsymbol{\sigma}\cdot\mathbf{r}\right|^2\left\{\frac{f_0g_0'-f_{-2}'g_{-2}}{\rho^2}-\frac{K}{3}\left[\frac{(f_0+f_0'\rho)f_0+(g_{-2}+g_{-2}'\rho)g_{-2}}{3\rho^2}-\frac{g_0g_0'+f_{-2}f_{-2}'}{\rho}\right]\right\}\right.$$
$$\left.+i\int\boldsymbol{\sigma}\cdot\mathbf{r}\left(\int\beta\gamma_5\right)^*\left\{\frac{f_0g_0-f_{-2}g_{-2}}{\rho}-\frac{K}{3}[\tfrac{1}{3}(f_0^2+g_{-2}^2)-(g_0^2+f_{-2}^2)]\right\}2M\right\}=C_{tp}{}^{10}\cdot 2p^2F.$$

TABLE II. Correction factors for parity change transitions: $\Delta I=0,\ \pm1,\ \pm2$; no $0\to0$, $\tfrac{1}{2}\to\tfrac{1}{2}$, $0\leftrightarrow1$, (yes).

$$G_p'^2\frac{3}{4}\left\{\sum_{i,j}|E_{ij}|^2\left\{\frac{f_2'^2+g_{-2}'^2}{\rho^2}+\frac{K^2}{9}\left[\frac{(f_0+f_0'\rho)^2+(g_{-2}+g_{-2}'\rho)^2}{\rho^2}\right]\right\}+2i\sum_{i,j}E_{ij}(F_{ij})^*\left\{\frac{f_1f_1'+g_{-2}g_{-2}'}{\rho}+\frac{K^2}{9}[(f_0+f_0'\rho)f_0+(g_{-2}+g_{-2}'\rho)g_{-2}]\right\}2M\right.$$
$$\left.+\sum_{i,j}|F_{ij}|^2\left\{f_1^2+g_{-2}^2+\frac{K^2}{9}[f_0^2+g_{-2}^2]\rho^2\right\}4M^2\right\}=C_{pp}{}^{12}\cdot 2p^2F.$$

$$2G_aG_p\frac{3}{4}\left\{\sum_{i,j}B_{ij}(E_{ij})^*\frac{K}{9}\left[-\frac{(f_0+f_0'\rho)f_0-(g_{-2}+g_{-2}'\rho)g_{-2}}{\rho^2}\right]+i\sum_{i,j}B_{ij}(F_{ij})^*\frac{K}{9}[-(f_0^2-g_{-2}^2)]2M\right.$$
$$+i\sum_{i,j}G_{ij}(E_{ij})^*\left\{-\frac{f_1f_1'-g_{-2}g_{-2}'}{\rho}-\frac{K^2}{9}[(f_0+f_0'\rho)f_0-(g_{-2}+g_{-2}'\rho)g_{-2}]+\sum_{i,j}G_{ij}(F_{ij})^*\left[f_1^2-g_{-2}^2+\frac{K}{9}(f_0^2-g_{-2}^2)\rho^2\right]2M\right\}=C_{ap}{}'^2\cdot 2p^2F.$$
$$2G_tG_p'\frac{3}{4}\left\{\sum_{i,j}B_{ij}(E_{ij})^*\frac{K}{9}\left[-\frac{(f_0+f_0'\rho)f_0+(g_{-2}+g_{-2}'\rho)g_{-2}}{\rho^2}\right]+i\sum_{i,j}B_{ij}(F_{ij})^*\frac{K}{9}[-(f_0^2+g_{-2}^2)]2M\right\}=C_{tp}{}'^2\cdot 2p^2F.$$

instead of the single matrix element, $\int\theta_p\gamma_5$.[1,2] An earlier paper[3] deals with these expressions as applied to $\Delta I=0$, (yes) transitions.

A check on the above method is provided by the calculation of the pseudoscalar transition matrix element in the one-nucleon representation of the initial and final states. Here,

$$ME_p^{(1)}=G_p\int(-\chi_f{}^\dagger(\boldsymbol{\sigma}'\cdot\mathbf{p}+V_3+\boldsymbol{\sigma}\cdot\mathbf{V}_4)$$
$$\times(W_f+2M+V_1+\boldsymbol{\sigma}'\cdot\mathbf{V}_2)^{-1})Q\begin{pmatrix}0 & L_p\\ -L_p & 0\end{pmatrix}$$
$$\times(-(W_i+2M+V_1+\boldsymbol{\sigma}'\cdot\mathbf{V}_2)^{-1}$$
$$\times(\boldsymbol{\sigma}'\cdot\mathbf{p}+V_3+\boldsymbol{\sigma}'\cdot\mathbf{V}_4)\chi_i)d\tau,\quad(11)$$

[1] E. J. Konopinski and G. E. Uhlenbeck, Phys. Rev. 60, 308 (1941).
[2] A. M. Smith, Phys. Rev. 82, 955 (1951).
[3] Ahrens, Feenberg, and Primakoff, Phys. Rev. 87, 663 (1952); referred to as I.

in terms of the one-nucleon large spinor components χ; the connection of $ME_p^{(1)}$ to the general ME_p is given by the independent particle model. In Eq. (11) $V_{1,2,3,4}$ denote combinations of the one-nucleon potentials due to all five covariant interactions;[4] σ' is Pauli's spin operator. Expanding in ascending powers of

$$(W+V_1+\sigma'\cdot\mathbf{V}_2)/2M,$$

and dropping all but the first two terms, yields

$$ME_p^{(1)}=\int\{\chi_f(\sigma'\cdot\mathbf{p}+V_3+\sigma'\cdot\mathbf{V}_4)$$
$$\times[-L_p/2M+(W_f+V_1+\sigma'\cdot\mathbf{V}_2)L_p/4M^2]$$
$$-[-L_p/2M+L_p(W_i+\sigma'\cdot\mathbf{V}_2)/4M^2]$$
$$\times(\sigma'\cdot\mathbf{p}+V_3+\sigma'\cdot\mathbf{V}_4)\chi_i\}dv, \quad (12)$$

which, assuming again that the $V_{1,2,3,4}$ are velocity independent, permits the derivation of the partially relativistic approximation to

$$(f|\beta\gamma_5\theta_p|i)R_a]_\rho+i(f|\theta_p\sigma\cdot\{\nabla|i)R_p\}_\rho/2M, \quad (13)$$

in agreement with Eqs. (9) and (10).

3. APPLICATION OF THEORY TO PARITY CHANGE BETA-DECAY

The result of applying the above theory to parity change transitions is exhibited in Tables I and II in the form of a pseudoscalar square correction factor and of tensor pseudoscalar and axial-vector pseudoscalar cross-correction factors. The new symbols in the tables are defined as

$$E_{ij}=\int\sigma\cdot\mathbf{r}\frac{2r_ir_j-\frac{2}{3}r^2\delta_{ij}}{r^2}, \quad F_{ij}=\int\beta\gamma_5\frac{2r_ir_j-\frac{2}{3}r^2\delta_{ij}}{r^2},$$
$$G_{ij}=\int\gamma_5\frac{2r_ir_j-\frac{2}{3}r^2\delta_{ij}}{r^2}, \quad G_p'=\frac{G_p}{2M}.$$

Evaluation of the terms containing Coulomb functions and their derivatives may then start with the relations,

$$f_{-K-1}=-\left(W-1+\frac{\alpha Z}{r}\right)g_{-K-1}+\frac{(K-1)}{r}\cdot f_{-K-1},$$

and

$$g_{-K-1}=\left(W+1+\frac{\alpha Z}{r}\right)f_{-K-1}-\frac{(K+1)}{r}g_{-K-1};$$

the resulting f_{-K-1}^2, g_{-K-1}^2, and $f_{-K-1}\times g_{-K-1}$ being obtained by using the expressions L, M, and N,[1,2] or, if the order to which the latter are carried is insufficient, by using ($\alpha=1/137$)

$$f_{-K-1}^2=A^2r^{2(\gamma-1)}(W-1)\left\{S-\frac{2}{2\gamma+1}(2S\alpha ZW-ap)r\right.$$
$$+\frac{2}{(2\gamma+1)^2(\gamma+1)}[S\alpha^2Z^2(4\gamma+3)W^2$$
$$-a\alpha Z(4\gamma+3)pW-S(1+\gamma)^2p^2$$
$$\left.+(1+\gamma)(\delta^2+\gamma^2)p^2]r^2\right\},$$

$$g_{-K-1}^2=A^2r^{2(\gamma-1)}(W+1)\left\{\mathcal{O}-\frac{2}{2\gamma+1}(2\mathcal{O}\alpha ZW+ap)r\right.$$
$$+\frac{2}{(2\gamma+1)^2(\gamma+1)}[\mathcal{O}\alpha^2Z^2(4\gamma+3)W^2$$
$$+a\alpha Z(4\gamma+3)pW-\mathcal{O}(1+\gamma)^2p^2$$
$$\left.+(1+\gamma)(\delta^2+\gamma^2)p^2]r^2\right\},$$

$$f_{-K-1}g_{-K-1}=A^2r^{2(\gamma-1)}p\left\{-a+\frac{2}{2\gamma+1}(2a\alpha ZW+bp)r\right.$$
$$-\frac{2}{(2\gamma+1)^2(\gamma+1)}[a\alpha^2Z^2(4\gamma+3)W^2$$
$$\left.+b\alpha Z(4\gamma+3)W-a(1+\gamma)^2p^2]r^2\right\},$$

where $A=e^{\pi\delta/2}|\Gamma(\gamma+i\delta)|(2p)^\gamma/(2W)^{\frac{1}{2}}\Gamma(2\gamma+1)$; thus, e.g., $F=2A^2Wp^{2(s-1)}/p^2$ with $|K|=1$ and

$$F_1=72A^2W^{2(s_1-2)}/p^4$$

with $|K|=2$, $s_1=4-(Z/137)^2$, $\gamma=K^2-(Z/137)^2$.[5]

$$a=\delta(\gamma/W-K), \quad b=K\gamma+\delta^2/W,$$
$$S=\delta^2(1+1/W)+\gamma(\gamma+K), \quad \mathcal{O}=\delta^2(1-1/W)+\gamma(\gamma-K).$$

4. PLANE WAVE APPROXIMATION

As a check it is opportune to perform a plane wave treatment of the lepton covariant. Because of the simple structure of the individual terms within the exponential function of the plane wave, the evaluation of the radial part of the lepton covariant at the boundary of the nucleus would not be necessary if it were not for the particular property of the pseudoscalar interaction to possess in the Coulomb treatment two sets of nuclear matrix elements instead of one; therefore to obtain manifest agreement with the results of the Coulomb calculations the plane wave calculations must also employ relation (9) (without the last term). This was done and agreement achieved with the $Z=0$ limit of the expressions in Tables I and II, upon addition of some third- and fourth-order terms in ρ; these last

[4] From a generalized one-nucleon Dirac equation,
$$(-\alpha\cdot\mathbf{p}-\beta M-\beta V_s-1V_v^{(1)}+\alpha\cdot\mathbf{V}_v^{(\alpha)}-\beta\sigma\cdot\mathbf{V}_t^{(\beta\sigma)}-\beta\alpha\cdot\mathbf{V}_t^{(\beta\alpha)}$$
$$-\sigma\cdot\mathbf{V}_a^{(\sigma)}+\gamma_5V_a^{(\gamma_5)}-\beta\gamma_5V_p)\psi=(W+M)\psi;$$
and, with $\psi=\binom{\chi'}{\chi}$, one obtains $V_1=V_s+V_v^{(1)}$; $V_2=V_t^{(\beta\sigma)}+V_a^{(\sigma)}$; $V_3=V_p-V_a^{(\gamma_5)}$; $V_4=V_t^{(\beta\alpha)}-V_v^{(\alpha)}$.

[5] M. E. Rose, Phys. Rev. 51, 484 (1937).

however are very small and were not entered in the tables.

5. CONCLUSION

The foregoing should enable correct treatment of first forbidden transitions with an arbitrary amount of pseudoscalar admixture. This is at present particularly valuable in the case of the decay of RaE; there, however, additional corrections due to the finite size of the nucleus must be calculated.

The author wishes to thank Professors E. Feenberg and H. Primakoff sincerely for suggesting this work and for extending their advice.

Technical Report No. 116

December 16, 1953

ANGULAR CORRELATION BETWEEN THE FIRST AND THIRD GAMMA RAYS Ti^{48}

By

C. E Whittle and P. S. Jastram

Reprinted from THE PHYSICAL REVIEW, Vol. 92, No. 1, 205-206, October 1, 1953
Printed in U. S. A

Angular Correlation between the First and Third Gamma Rays in Ti^{48}†

C. E. WHITTLE AND P. S. JASTRAM
Washington University, St. Louis, Missouri
(Received August 3, 1953)

THE angular correlation function for the cascaded gamma rays of 1.32 and 0.99 Mev in Ti^{48} that follow the positron decay of V^{48} has previously been reported.[1] The measurement has since been repeated by two independent investigations,[2,3] results of which confirm the spin assignment 0–2–4 for the first three levels of Ti^{48}. In addition, negatron decay of Sc^{48} is found[4,5] to yield a third excited level in Ti^{48}, lying about 1.05 Mev higher than the second excited state. On comparing the gamma-ray spectra of Sc^{48} and V^{48} in a scintillation spectrometer we find, in agreement with Sterk *et al.*,[5] that the 1-Mev peak is broader and has its maximum displaced to a slightly higher energy for the scandium than for the vanadium. This indicates the presence of an additional gamma ray in the scandium decay, of slightly higher energy than the 0.99-Mev quantum but too close to be resolved as a separate line in the scintillation spectrometer. Measurement of the coincidence rate between the 1-Mev and 1.32-Mev peaks, with suitable normalization for single counting rates and use of an empirically determined correction for variation of scintillation counter efficiency with energy, has confirmed the result of Hamermesh *et al.*[4] that the 1.05-Mev line in the scandium decay is in cascade with the 0.99- and 1.32-Mev photons. The experiments of Peiper[6] and Harvey,[7] using respectively *d-p* and *p-p* reactions to determine the nuclear energy levels in Ti^{48}, give further support for these results and fix the order of the gamma rays to be, in order of emission, 1.05, 1.32, and 0.99 Mev.

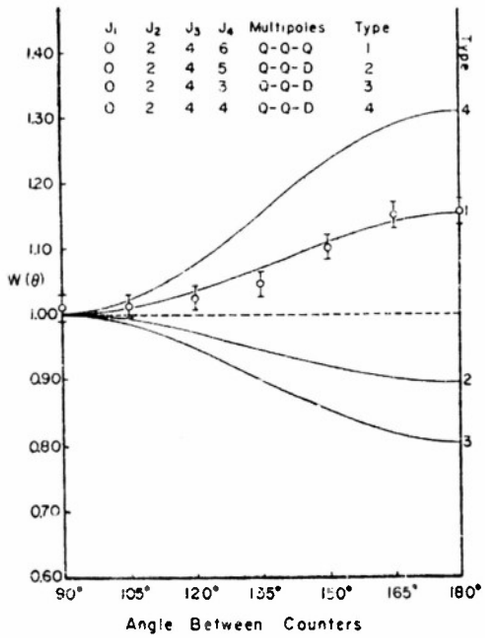

FIG. 1. The angular correlation between the first and third gamma rays in Ti^{48}. Comparison of the experimental points with curves plotted for values of the P_2 and P_4 coefficients given by Arfken, Biedenharn, and Rose for four possible choices of the spin of the third excited state in Ti^{48} establishes that this level has spin 6 and decays by quadrupole radiation.

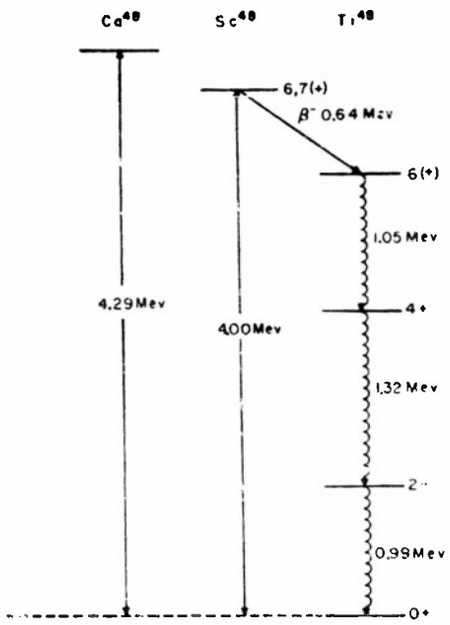

FIG. 2. Decay scheme of Sc^{48}. All spin, parity, and energy values are experimentally determined except the parity of the 3.36-Mev titanium level and the scandium ground state. The Ca^{48} ground state is included to show its position relative to the Sc^{48} ground state.

We have measured the angular correlation function between the first and third gamma rays. The experimental arrangement used was similar to that described in reference 1, except that NaI(Tl) scintillators and differential pulse height selectors were used in order to accept only pulses in the 1-Mev peak. Coincidence rates were determined with one of the pulse-height channels set below and then above the 1-Mev peak, in order to insure that the measured coincidence rate and corresponding angular correlation was not between "1-Mev" lines and the 1.32-Mev Compton distribution, the end point of which lies at 1.1 Mev. The points in Fig. 1 show the 0.99–1.05 Mev coincidence rate as a function of the angle. The data are in agreement with the distribution[8]

$$W(\theta)=1+0.102P_2(\cos\theta)+0.0091P_4(\cos\theta),$$

which holds when all three gamma rays are quadrupole and for spin assignments 0–2–4–6 for the ground state and first three excited states of Ti^{48}. The same distribution is predicted for any

order of the gamma rays; hence this is a case in which the first and third gamma-ray correlation cannot determine the order of emission. Curves computed by use of the coefficients given by Arfken, Biedenharn, and Rose[8] are shown for other possible values of spin for the third excited state.

Kurath[9] has pointed out that in the shell model based on *jj* coupling and static central-force interactions between nucleons, a nucleus such as $_{21}Sc^{48}$, with 1 proton and one neutron-hole in the $1f_{7/2}$ level, should have a ground-state spin of either the maximum possible value or one less than the maximum. The spins of the first four Ti^{48} levels, together with the allowed classification[10] of the 0.64-Mev beta decay of Sc^{48} and the absence of higher energy groups, require that the Sc^{48} ground-state spin be either 6 or 7, in full agreement with Kurath's prediction. The experimental evidence does not indicate which spin is the more likely.

On the basis of the polarization-direction correlation[11] between the 0.99- and 1.32-Mev photons, even parity is assigned to the first two excited levels in Ti^{48}. Direct evidence for the parity of the 3.36-Mev level is lacking, but in view of the allowed nature of the scandium beta decay and the probable shell-model assignment of even parity to the Sc^{48} ground state, it is probably also even. The decay scheme of Sc^{48} consistent with all evidence reported to date is shown in Fig. 2.

† Assisted by the joint program of the U. S. Office of Naval Research and the U. S. Atomic Energy Commission.

[1] P. S. Jastram and C. E. Whittle, Phys. Rev. **87**, 1133 (1952).
[2] Roggenkamp, Pruett, and Wilkinson, Phys. Rev. **88**, 1262 (1952).
[3] P. Meyer and S. Schlieder, Z. Physik **135**, 119 (1953).
[4] Hamermesh, Hummel, Goodman, and Engelkemeir, Phys. Rev. **87**, 528 (1952).
[5] Sterk, Wapstra, and Kropveld, Physica **19**, 135 (1953).
[6] G. F. Pelper, Phys. Rev. **88**, 1269 (1952).
[7] J. A. Harvey, Phys. Rev. **88**, 162 (1952).
[8] Arfken, Biedenharn, and Rose, Phys. Rev. **86**, 761 (1952).
[9] D. Kurath, Phys. Rev. **87**, 528 (1952).
[10] E. Feenberg and G. Trigg, Revs. Modern Phys. **22**, 406 (1950).
[11] C. E. Whittle and P. S. Jastram (to be published).

Technical Report No. 117

December 16, 1953

PROTON-DEUTERON SCATTERING AT 5.1 MEV AND DEUTERON-PROTON SCATTERING AT 10.2 MEV.

By

K. B. Mather

PROTON-DEUTERON SCATTERING AT 5.1 MEV AND DEUTERON-PROTON SCATTERING AT 10.2 MEV.*

K. B. Mather**

Washington University, Dept. of Physics, St. Louis, Missouri.

ABSTRACT

A photographic scattering chamber has been used to study the elastic scattering of 5.1-Mev protons by deuterium and 10.2 Mev deuterons by hydrogen, these being the same process in the center-of-mass system. Differential cross sections were obtained from 16.4° to 172.9°. These are in good agreement with other experimental data at about the same energy. Comparison is made with the theoretical angular distribution due to Buckingham, Hubbard, and Massey, based on a symmetrical exchange force. Agreement is close at this energy, favoring exchange rather than ordinary force theories. However, at higher energies (~ 10-Mev p-d) the BHM calculations do not represent the interaction satisfactorily.

---

*The experimental portion of this work was conducted at Washington University, St. Louis, Mo. assisted by the ONR and the AEC.

** Now with the Commonwealth Scientific and Industrial Research Organization, Physics Department, University of Melbourne, Melbourne, Australia.

I. INTRODUCTION

The proton-deuteron interaction has now been studied at various energies from 250 kev to 10 Mev, including three studies at approximately 5 Mev.[1] The present report contributes

1. R. F. Taschek, Phys. Rev. 61, 13 (1942), 250 and 275 kev; Tuve, Heydenberg, and Hafsted, Phys. Rev. 50, 806 (1936), 830 kev; Sherr, Blair, Kratz, Bailey and Taschek, Phys. Rev. 72, 662 (1947), 1.51, 2.08, 2.53, 3.00, and 3.49 Mev; Heitler, May, and Powell, Proc. Roy. Soc. (London) A190, 180 (1947), 4.2 Mev; Rodgers, Leiter, and Kruger, Phys. Rev. 78, 656 (1950), 4.97 Mev; Karr, Bondelid, and Mather, Phys. Rev. 81, 37 (1950), 5.0 Mev; L. Rosen and J. C. Allred, Phys. Rev. 82, 777 (1951), 5.2 Mev; Armstrong, Allred, Bondelid, and Rosen, Phys. Rev. 83, 218 (1951), 9.7 Mev.

further data at 5.1 Mev over a somewhat wider range of angles. The data were acquired by scattering both 5.1-Mev protons from deuterium and 10.2-Mev deuterons from hydrogen, the combination of the techniques having obvious advantages in revealing special errors to which either one is liable.

II. METHOD

The apparatus employed consisted of the photographic scattering chamber described in an earlier publication[2] on proton-proton

2. K. B. Mather, Phys. Rev. 82, 133 (1951).

scattering, and its manner of use was essentially unchanged in the present work. However, in p-d scattering, scattered and recoil particles are different and distinguishable and were counted separately, leading to the differential scattering cross section in the laboratory system by the following formula:[3]

3. This formula appeared incorrectly in reference 2. The symbols are defined there.

$$\sigma(\theta) = n_\alpha Rh \sin\theta / N_{cc} N_i 2b \sin\phi$$

Conversion to center-of-mass cross section $\sigma(\theta)$ at center-of-mass angle θ is achieved by formulas:

$$\sigma(\theta) = \sigma(\theta_1) \cdot (\sin\theta_1/\sin\theta)^2 \cdot \cos(\theta - \theta_1)$$

if scattered tracks at angle θ_1 are counted, and

$$\sigma(\theta) = \sigma(\theta_2)/4 \cos\theta_2$$

if recoil tracks at angle θ_2 are counted, the angle relationship being

$$\theta = (\pi - 2\theta_2).$$

In p-d scattering the proton may be scattered at all laboratory angles from 0 to 180° the deuteron recoiling at angle from 0 to 90°. In d-p scattering the deuteron has a maximum angle of scatter of 30°, the proton recoiling at angles from 0 to 90°. Owing to the fact that there are two kinds of collision (hard and soft) which can scatter the deuteron at any angle less than 30°, three distinct track lengths appear in the photographic emulsion at all angles below 30° -- a short deuteron track, a long deuteron track, and a recoil proton track.

Approximate ranges in Nuclear Research Emulsions (Ilford C2) are listed in column 4 of Tables I and II, for p-d and d-p cases, respectively. It will be observed that it is always possible and generally easy to distinguish, by their ranges, the several particles which appear at any angle. The fact that one plate can, for d-p scattering below 30°, yield three scattering cross sections endows the method with special merit. These three values serve as related "triplets" since they derive from the same slit unit

and precisely the same geometry is used in computing them. They should therefore be very reliable in relative value. Similarly, in p-d scattering below 90° there are related "doublets."

III. EXPERIMENTAL DETAILS

The source of protons and deuterons was the Washington University 45-inch cyclotron. The beam energy was redetermined during every run by measuring ranges in a photographic plate placed at the 45° position at a small angle, $\Phi = 3°$. The range-energy data of Rotblat[4] were used, leading to average energy values

4. J. Rotblat, Nature 167, 550 (1951).

at the scattering volume of 5.1 ± 0.1 Mev for the protons and 10.2 ± 0.2 Mev for the deuterons, in the laboratory system.

The energy of each individual run could be stated rather more precisely than this but as the beam energy appeared to vary slightly from run to run, average values have been quoted together with uncertainties which cover the extreme limits encountered.

The deuterium and hydrogen used as scattering gases were 99.5 and 99.8 percent pure, respectively. Experiments were usually conducted at a gas pressure of approximately 1.4 cm Hg which was low enough to prevent any serious multiple scattering effects.

The p-d data were much "cleaner" than the d-p due particularly to the heavy neutron flux which is always associated with a cyclotron accelerating deuterons. During preliminary runs it was found that the background on the plates due to knock-on protons was heavy and would have complicated the scanning unnecessarily. This was reduced to a few percent by surrounding the scattering chamber with a concrete fort 16 inches thick on the side facing the cyclotron and reinforced about the collimator with timber blocks.

Runs were made at several different exposures so as to give optimum track density over each range of angles to facilitate scanning. The method of scanning was the same as described in reference 2. In certain cases, however, e.g., d-p runs 5 and 6, for $\theta < 30^\circ$, only short deuteron tracks were counted as these could be counted quickly. Counting long deuterons and protons was more tedious, requiring ideal exposure conditions, and was only considered worthwhile for run 7.

IV. RESULTS AND DISCUSSION

The final values of seven runs are listed in Table I (p-d) and Table II (d-p) ranging from $\theta = 16.4^\circ$ to 172.9°, and all data are shown in Fig. 1 as $\sigma(\theta)$ versus θ. The total number of tracks counted was 105,500. The number contributing to each value is given in parentheses after the value and determines the standard deviation of the value imposed by the counting. Other errors are the same as listed in Sec. VIII of reference 2. The probable error in relative values, excluding the statistical error, is ~ 0.4 percent.

Corrections had to be applied to the p-d data as follows: (1) Scattering volume. This is not exactly the same as implied in the formula for $\sigma(\theta)$ in Sec. II. A correction had to be applied only at $\theta = 165^\circ$ and amounted to 0.7 percent. (2) Air leakage, degassing of plates and equipment, and impure gas. This amounted to ~ 5 percent at $\theta = 11^\circ$ and declined rapidly at larger angles. (3) Slit width. This applied only where the cross section was changing rapidly, viz., at small laboratory angles where it amounted in several cases to a few percent.

Similar corrections pertained to the d-p runs. On the whole, the p-d scanning was more straightforward. Fewer cases of ambiguous track lengths occurred and hence runs 1 and 2 should carry rather more weight.

In run 6 the tracks were so congested that only short deuteron tracks could be counted confidently and even there it was felt that some tracks might be overlooked. This may account for the tendency towards lower values in this run. The d-p data show considerable scatter at $\theta = 30^\circ$ to 40°. This is due to the difficulty of counting accurately the short proton tracks, especially at 30°. These tracks are only 7μ in mean range and, allowing for straggling, some of the tracks are too short to be established with certainty. In run 4 the value at 30° is a lower limit. About 10 percent more "probables" were recorded and it seems likely that others escaped notice altogether.

Beyond about 160° the same trouble operates. Some short deuterons, especially at $\theta = 168.6^\circ$ and 172.9° may be missed. The p-d data which have better statistics in this region would be expected to suffer from the same cause but seem to be rather higher in value. Probably the curve begins to flatten off at or near 160° as predicted by the Buckingham, Hubbard, and Massey theory, but this region is difficult to study and the present data are not conclusive beyond about 160°.

Moreover, where this error exists, multiple scattering losses will also be at their worse and due to the complicated "compensating" mechanism (see Sec. VIII of reference 2) it is very difficult to estimate the consequences. Lower limit values are prefixed in the tables by ℓ. Other values which are suspected for any reason (poor scanning conditions, heavy background, etc.) are prefixed by x.

In the present work absolute values were determined by two methods: (a) By measuring the charge collected on a standard condenser as described in the earlier publications. (b) By assuming a value for the absolute cross section of p-p scattering (which is established to a higher degree of precision than any other scattering process) and determining p-d and d-p cross sections relative to p-p. The reason for introducing (b) is that as a result of a recheck by the Bureau of Standards some doubts have arisen concerning the true values of the condensers at the time this work was carried out.

Cross sections were therefore determined relative to the p-p results of reference 2, which appear to be consistent with other results at or near this energy; i.e., assuming absolute p-p cross sections to be in accordance with pure S-wave scattering of phase shift $\delta_0 = 54.5°$. The derived absolute p-d and d-p cross sections agreed with those measured directly (method (a)) to ~ 2 percent. The cross sections in Tables I and II are the mean of both methods and are believed to have an accuracy in absolute value of ± 2 percent (probable error) taking account of all sources of systematic error which have been recognized but not including the effect of statistical error on the individual values.

In Fig. 1 all the experimental points of the present work have been plotted. The point at $\theta = 16.4°$ is uncertain but seems to be consistent with purely Rutherford-Darwin scattering indicating that the scattering is essentially Coulombian below this angle. The minimum cross section at this energy occurs at approximately $112°$ in the center-of-mass system.

The full curve (BHM) represents the calculated angular distribution of 5-Mev protons due to Buckingham et al.[5] based on a symmetrical exchange force as in the earlier work of Buckingham and Massey, but including allowance for D-wave scattering. The new calculations are markedly superior in representing the observations at large angles (see comparison with earlier theory made by Karr et al., reference 1) and appear to represent the experimental facts of p-d scattering fairly satisfactorily from about 2 to 5 Mev. In absolute value at 5 Mev the theoretical curve would fit the data better if ~9 percent lower.

However, the recent p-d scattering at 9.7 Mev carried out at Los Alamos by Armstrong et al. (see reference 1) can be compared roughly with the BHM calculations at 11.5 Mev and here the agreement is poor. The experimental curve rises much more steeply at large angles and also shows no tendency to flatten off between about 30° and 60° as predicted by BHM. These discrepancies seem to be paralleled also by high energy n-d scattering.

Part of the scanning involved in this project was carried out at Birmingham University, England, assisted by an Imperial Chemical Industries Fellowship.

5. Buckingham, Hubbard, and Massey, Proc. Roy Soc. (London) A211, 183 (1952).

FIGURE 1.

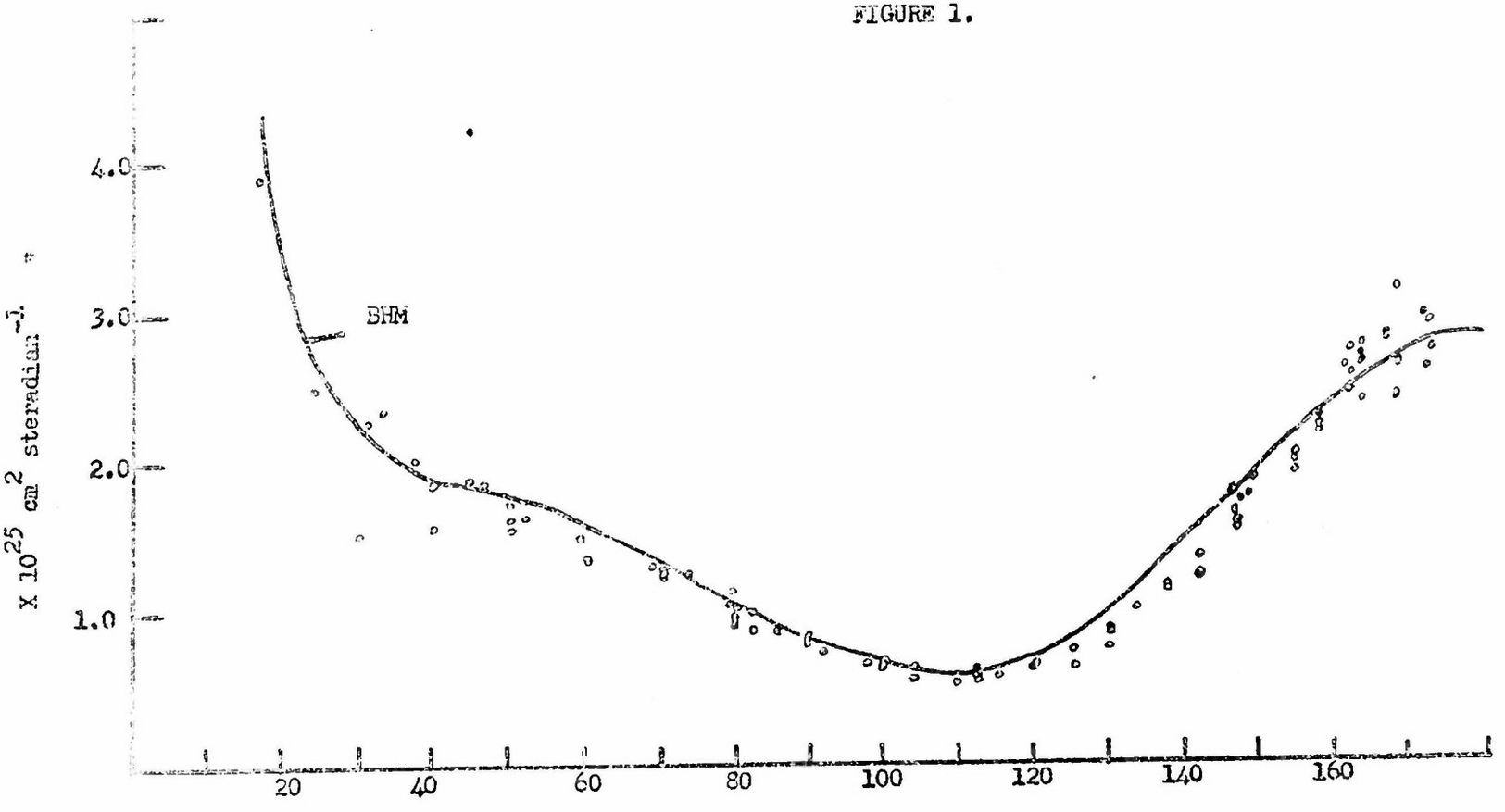
4.0
3.0
2.0
1.0
BHM
X 10^25 cm^2 steradian^-1
20
40
60
80
100
120
140
160
SCATTERING ANGLE θ IN CM SYSTEM

TABLE 1. DIFFERENTIAL CROSS SECTIONS DERIVED FROM TWO p-d SCATTERING RUNS AT 5.1 Mev. THE FIGURES IN PARENTHESIS ARE NUMBERS OF TRACKS CONTRIBUTING TO THE VALUES. IN THE THIRD COLUMN, p INDICATES SCATTERED PROTON AND d RECOIL DEUTERON.

Θ_c	Θ	Kind of track	Range in μ	$\sigma(\theta) \times 10^{25}$ cm^2 steradian^{-1} Run 1		Run 2	
11	16.4	p	168	~3.90	(1200)		
	156.0	d	89	2.29	(1212)		
15	22.4	p	162				
	150.0	d	84				
16	23.9	p	162	2.48	(1158)		
	148.0	d	83	1.72	(1355)		
21	31.1	p	155	2.27	(966)		
	138.0	d	77	1.17	(845)		
25	37.2	p	148	2.00	(1733)		
	130.0	d	71	0.846	(1245)		
30	44.5	p	138	1.86	(735)		
	120.0	d	61	0.602	(401)		
35	51.7	p	129	1.63	(1242)		
	110.0	d	52	0.533	(680)		
40	58.7	p	118	1.47	(1294)	1.49	(1207)
	100.0	d	42	0.646	(911)	0.631	(841)
45	65.7	p	106				
	90.0	d	33			0.84	(188)
50	73.5	p	92	1.11	(968)		
	80.0	d	26	1.00	(1205)		
55	79.2	p	82	1.02	(721)	1.12	(861)
	70.0	d	19	1.25	(1294)	1.24	(1382)
60	85.6	p	71			0.862	(1200)
	60.0	d	13			1.37	(2570)
65	91.9	p	62	0.743	(611)	0.734	(919)
	50.0	d	8	1.71	(1736)	1.60	(2457)
70	40.0	d	5			0.651	(1112)
75	103.9	p	48	0.550	(511)	0.616	(1006)
	30.0	d	~3				
85	114.9	p	35			0.577	(1037)
	10.0	d	- -				

Continued on next page

TABLE I. (continued)

[illegible]	[illegible]	Kind of track	Range in μ	$\sigma(\theta)$ x 10^{25} cm^2 steradian^{-1} Run 1		Run 2	
95	124.5	p	26	0.618	(367)	0.712	(990)
105	133.8	p	19			1.01	(1121)
115	141.9	p	15	1.24	(534)	1.36	(1141)
125	149.1	p	12			1.77	(1305)
135	155.7	p	10			2.22	(1028)
145	161.6	p	8			2.60	(1240)
155	167.2	p	7			2.84	(1217)
165	172.4	p	~7			2.96	(2488)

TABLE [illegible]. DIFFERENTIAL CROSS SECTIONS DERIVED FROM FIVE d-p SCATTERING RUNS AT 10.2 Mev. IN THE THIRD COLUMN ℓd INDICATES DEUTERON TRACK, sd SHORT DEUTERON TRACK AND p RECOIL PROTON TRACK. PREFIX ℓ INDICATES LOWER LIMIT VALUE AND ≈ DOUBTFUL VALUE.

Θ	φ	Kind of track	Range in μ	$\sigma(\Theta) \times 10^{25}$ cm^2 steradian^{-1} Run 3		Run 4		Run 5		Run 6		Run 7	
7	21.1	ℓd	325										
	166.0	p	440										
	172.9	sd	13					ℓ2.73	(532)	ℓ2.6	(118)	ℓ2.9	(314)
												2.32	(430)
11	33.4	ℓd	300									2.31	(187)
	158.0	p	425										
	168.6	sd	15					ℓ2.68	(1120)	ℓ2.42	(996)	ℓ3.11	(81)
												1.82	(1129)
15	46.1	ℓd	264									1.91	(504)
	150.0	p	403										
	163.9	sd	16	2.63	(889)			2.69	(1536)	2.40	(1859)	2.74	(262)
16	49.4	ℓd	260										
	148.0	p	396										
	162.5	sd	16	2.57	(946)			2.49	(1320)			2.70	(724)
												1.30	(1132)
21	66.8	ℓd	238									1.14	(390)
	138.0	p	359										
	155.2	sd	20					1.92	(1404)	1.99	(488)	2.04	(375)
												0.875	(1709)
25	82.7	ℓd	196			0.954	(1236)					0.752	(544)
	130.0	p	324			0.839	(384)						
	147.3	sd	25			1.80	(722)	≈1.58	(994)	1.66	(1280)	1.60	(973)
30	120.0	p	276			0.639	(316)						
35	110.0	p	230	0.536	(1903)	0.563	(1070)	0.545	(2400)			0.610	(1049)
40	100.0	p	184	0.637	(2180)	0.613	(739)	0.622	(2267)			0.666	(1075)
45	90.0	p	141	0.780	(291)								
50	80.0	p	104	0.957	(2365)	0.945	(1047)	0.879	(2488)				
55	70.0	p	70					1.21	(2906)				
60	60.0	p	47					1.34	(1828)				
65	50.0	p	28	1.55	(2270)			≈1.56	(2392)				
70	40.0	p	15	1.85	(1918)			1.58	(1905)				
75	30.0	p	7			ℓ1.52	(220)						

N U C L E A R P H Y S I C S

Technical and Final Report Distribution List

1 October 1953

Professional

Dr. W. F. G. Swann, Director
Bartol Research Foundation
Franklin Institute
Swarthmore, Pennsylvania

Prof. C. C. Lauritsen
Department of Physics
California Institute of Technology
Pasadena, California

Prof. C. D. Anderson
Department of Physics
California Institute of Technology
Pasadena, California

Prof. R. B. Brode
Department of Physics
University of California
Berkeley 4, California

Prof. E. O. Lawrence
Radiation Laboratory
University of California
Berkeley 4, California

Prof. J. R. Richardson
Department of Physics
University of California (L. A.)
Los Angeles 24, California

Prof. E. C. Creutz
Department of Physics
Carnegie Institute of Technology
Schenley Park
Pittsburgh 13, Pennsylvania

Dr. M. A. Tuve
Department of Terrestrial Magnetism
Carnegie Institution of Washington
Washington, D. C.

Dr. R. S. Shankland
Case Institute of Technology
Department of Physics
University Circle
Cleveland 6, Ohio

Prof. S. K. Allison
Institute of Nuclear Studies
University of Chicago
Chicago, Illinois

Prof. J. Rainwater
Columbia University
Nevis Cyclotron Laboratories
P. O. Box 117
Irvington-on Hudson, New York

Prof. R. R. Wilson
Laboratory of Nuclear Studies
Cornell University
Ithaca, New York

Prof. W. M. Nielsen
Department of Physics
Duke University
Durham, North Carolina

Dr. Guy Suits
Research Laboratory
General Electric Company
Schenectady, New York

Dr. Zoltan Bay
Department of Physics
George Washington University
Washington, D. C.

Prof. N. F. Ramsey
Department of Physics
Harvard University
Cambridge, Massachusetts

Director
Nuclear Laboratory
Harvard University
Cambridge, Massachusetts

Prof. F. W. Loomis
Department of Physics
University of Illinois
Urbana, Illinois

Prof. A. C. G. Mitchell
Department of Physics
Indiana University
Bloomington, Indiana

Prof. J. A. Van Allen
Dept. of Physics
State University of Iowa
Iowa City, Iowa

Prof. J. D. Stranathan
Department of Physics
University of Kansas
Lawrence, Kansas

Prof. J. M. Cork
Department of Physics
University of Michigan
Ann Arbor, Michigan

Prof. W. E. Hazen
Department of Physics
University of Michigan
Ann Arbor, Michigan

Prof. J. H. Williams
Department of Physics
University of Minnesota
Minneapolis, Minnesota

Prof. E. P. Ney
Department of Physics
University of Minnesota
Minneapolis, Minnesota

Prof. Truman S. Gray
Servo Mechanisms Laboratory
Massachusetts Institute of Technology
Cambridge 39, Massachusetts

Prof. J. R. Zacharias (2)
Laboratory for Nuclear Science and
Engineering
Massachusetts Institute of Technology
Cambridge 39, Massachusetts

Prof. S. A. Korff
Department of Physics
New York University
University Heights
New York 53, New York

Prof. B. Waldman
Nuclear Physics Laboratory
University of Notre Dame
Notre Dame, Indiana

Prof. J. N. Cooper
Department of Physics
Ohio State University
Columbus 10, Ohio

Prof. W. E. Stephens
Department of Physics
University of Pennsylvania
Philadelphia 4, Pennsylvania

Prof. A. J. Allen
Department of Physics
University of Pittsburgh
Pittsburgh, Pennsylvania

Prof. G. T. Reynolds
Department of Physics
Princeton University
Princeton, New Jersey

Prof. M. G. White
Department of Physics
Princeton University
Princeton, New Jersey

Prof. Leticia del Rosario
Department of Physics
Gobierno de Puerto Rico
Universidad de Puerto Rico
Rio Piedras
Puerto Rico

Prof. K. Lark-Horovitz
Department of Physics
Purdue University
Lafayette, Indiana

Prof. T. W. Bonner
Department of Physics
Rice Institute
Houston, Texas

Prof. R. E. Marshak
Department of Physics
University of Rochester
Rochester, New York

Prof. A. C. G. Mitchell
Department of Physics
Indiana University
Bloomington, Indiana

Prof. J. A. Van Allen
Dept. of Physics
State University of Iowa
Iowa City, Iowa

Prof. J. D. Stranathan
Department of Physics
University of Kansas
Lawrence, Kansas

Prof. J. M. Cork
Department of Physics
University of Michigan
Ann Arbor, Michigan

Prof. W. E. Hazen
Department of Physics
University of Michigan
Ann Arbor, Michigan

Prof. J. H. Williams
Department of Physics
University of Minnesota
Minneapolis, Minnesota

Prof. E. P. Ney
Department of Physics
University of Minnesota
Minneapolis, Minnesota

Prof. Truman S. Gray
Servo Mechanisms Laboratory
Massachusetts Institute of Technology
Cambridge 39, Massachusetts

Prof. J. R. Zacharias (2)
Laboratory for Nuclear Science and
Engineering
Massachusetts Institute of Technology
Cambridge 39, Massachusetts

Prof. S. A. Korff
Department of Physics
New York University
University Heights
New York 53, New York

Prof. B. Waldman
Nuclear Physics Laboratory
University of Notre Dame
Notre Dame, Indiana

Prof. J. N. Cooper
Department of Physics
Ohio State University
Columbus 10, Ohio

Prof. W. E. Stephens
Department of Physics
University of Pennsylvania
Philadelphia 4, Pennsylvania

Prof. A. J. Allen
Department of Physics
University of Pittsburgh
Pittsburgh, Pennsylvania

Prof. G. T. Reynolds
Department of Physics
Princeton University
Princeton, New Jersey

Prof. M. G. White
Department of Physics
Princeton University
Princeton, New Jersey

Prof. Leticia del Rosario
Department of Physics
Gobierno de Puerto Rico
Universidad de Puerto Rico
Rio Piedras
Puerto Rico

Prof. K. Lark-Horovitz
Department of Physics
Purdue University
Lafayette, Indiana

Prof. T. W. Bonner
Department of Physics
Rice Institute
Houston, Texas

Prof. R. L. Marshak
Department of Physics
University of Rochester
Rochester, New York

Prof. Charles A. Whitmer
Chairman, Department of Physics
Rutgers University
New Brunswick, New Jersey

Prof. E. L. Ginzton
Microwave Laboratory
Stanford University
Palo Alto, California

Prof. F. Bloch
Department of Physics
Stanford University
Palo Alto, California

Prof. J. D. Trimmer
Department of Physics
University of Tennessee
Knoxville, Tennessee

Prof. A. L. Hughes
Department of Physics
Washington University
St. Louis, Missouri

Prof. R. D. Sard
Department of Physics
Washington University
St. Louis, Missouri

Prof. J. H. Manley
Department of Physics
University of Washington
Seattle 5, Washington

Dr. J. W. Coltman
Research Laboratories
Westinghouse Electric Corporation
East Pittsburgh, Pennsylvania

Prof. R. C. Herb
Department of Physics
University of Wisconsin
Madison 6, Wisconsin

Prof. W. W. Watson (2)
Sloane Physics Laboratory
Yale University
New Haven 11, Connecticut

Governmental

Chief of Naval Research (2)
Attn: Nuclear Physics Branch
Department of the Navy
Washington 25, D. C.

Director, Naval Research Lab. (6)
Attn: Technical Information Officer
Washington 25, D. C.

Commanding Officer
Office of Naval Research
Chicago Branch Office
10th Flr., John Crerar Library Bldg.
86 East Randolph St.
Chicago 1, Illinois

Commanding Officer
Office of Naval Research
San Francisco Branch Office
1000 Geary St.
San Francisco, California

Commanding Officer
Office of Naval Research
New York Branch Office
346 Broadway, New York 13, N. Y.

Commanding Officer
Office of Naval Research
Pasadena Branch Office
1030 East Green St.
Pasadena 1, California

Commanding Officer (10)
Office of Naval Research
Navy No. 100
Fleet Post Office
New York, New York

Office of Technical Services
Department of Commerce
Washington 25, D. C.

Superintendent, Nucleonics Div.
Naval Research Laboratory
Anacostia, Washington, D. C.

Chief of the Bureau of Ships
Attn: Code 390
Department of the Navy
Washington 25, D. C.

Chief of the Bureau of Ships
Attn: Code 330
Department of the Navy
Washington 25, D. C.

Chief of the Bureau of Ordnance
Attn: Rem
Department of the Navy
Washington 25, D. C.

Chief of the Bureau of Ordnance
Attn: Re9a
Department of the Navy
Washington 25, D. C.

Chief of the Bureau of Aeronautics
Attn: RS-5
Department of the Navy
Washington 25, D. C.

Chief of the Bureau of Aeronautics
Attn: Technical Library
Department of the Navy
Washington 25, D. C.

Commanding Officer
Naval Radiological Defense Lab.
San Francisco Naval Shipyard
San Francisco 24, California

Armed Services Tech. Inf. Agency
Documents Service Center (5)
Knott Building
Dayton 2, Ohio

Chief of Naval Operations
Attn: Op 36
Navy Department
Washington 25, D. C.

Commander, U. S. Naval Ordnance Test Station
Technical Library
Inyokern, China Lake, California

Commanding General
Air Force Cambridge Research Center
Attn: Geophysics Research Library
230 Albany Street
Cambridge 39, Massachusetts

Senior Scientific Advisor
Office of the Under Secretary of the Army
Department of the Army
Washington 25, D. C.

Director, Research and Development Division
General Staff
Department of the Army
Washington 25, D. C.

Chief, Physics Branch
U. S. Atomic Energy Commission
1901 Constitution Avenue, N. W.
Washington 25, D. C.

U. S. Atomic Energy Commission
Attn: Roland Anderson
Patent Branch
1901 Constitution Avenue, N. W.
Washington 25, D. C.

U. S. Atomic Energy Commission
Library Branch
Technical Information Division,
P. O. Box E
Oak Ridge, Tennessee

Oak Ridge National Laboratory
Attn: Central Files
P. O. Box P
Oak Ridge, Tennessee

Oak Ridge National Laboratory
Attn: Head, Physics Division
P. O. Box P
Oak Ridge, Tennessee

Brookhaven National Laboratory
Attn: Dr. S. C. Stanford
Research Library
Upton, L. I., New York

Argonne National Laboratory
Attn: Hoylande D. Young
P. O. Box 5207
Chicago 80, Illinois

Document Custodian
Los Alamos Scientific Laboratory
P. O. Box 1663
Los Alamos, New Mexico

Technical Information Group
General Electric Company
P. O. Box 100
Richland, Washington

Carbide and Carbon Chemical Div.
(K-25 Plant)
Plant Records Department
Central Files (K-25)
P. O. Box P
Oak Ridge, Tennessee

Carbide and Carbon Chemical Div.
(Y-12 Plant)
Central Reports + Information (Y-1)
P. O. Box P
Oak Ridge, Tennessee

Ames Laboratory
Iowa State College
P. O. Box 14A, Station A
Ames, Iowa

Knolls Atomic Power Laboratory
Attn: Document Librarian
P. O. Box 1072
Schenectady, New York

Mound Laboratory
Attn: Dr. M. M Haring
U. S. Atomic Energy Commission
P. O. Box 32
Miamisburg, Ohio

Sandia Corporation
Sandia Base
Attn: Mr Dale M. Evans
Classified Document Division
Albuquerque, New Mexico

U. S. Atomic Energy Commission
Attn: Div. of Technical Information + Declassification Service
New York Operations Office
P. O. Box 30
Ansonia Station
New York 23, New York

National Bureau of Standards
Library
Room 203, Northwest Building
Washington 25, D. C.

Mr. Leonard Eyges
Scientific Attache, American Embassy
24 Rue Gabriel
Paris, France

Director, Office of Ordnance Research
2127 Myrtle Drive
Durham, North Carolina

Commanding General
Air Research and Development Command
Attn: RDRRP
P. O Box 1395
Baltimore 3, Maryland

Foreign

Senhor Cesar Lattes
Scientific Director
Brazilian Center of Physical Research
Rio de Janeiro, Brazil

Professor Hans Bethe
Department of Physics
Cornell University
Ithaca, New York

Dr. U. Fano
National Bureau of Standards
Washington 25, D. C.

Professor J. H. Reynolds
Department of Physics
University of California
Berkeley, California